Triple-Band Metasurface Absorber for RF Energy Harvesting Applications

Rajan Agrahari[1*], Satyesh Singh[1], Diptiranjan Samantaray[2], Bambam Kumar[1], Somak Bhattacharyya[2], Manpuran Mahto[1], and Pradip Kumar Jain[1]

***Abstract*—Energy harvesting is expected to be ubiquitous and essential to modern-day life in the future. The limitations of the ambient source such as thermal, mechanical, and solar for energy harvesting can be overcome by the RF energy harvesting for low power devices. With the help of perfect metasurface absorbers, an electromagnetic wave can be used as an ambient source for energy harvesting. In this paper, a simple polarization-insensitive triple-band perfect metasurface absorber is proposed for RF energy harvesting applications. The three-layer (metal-dielectric-metal) meta-atom of the designed metasurface consists of a cross-shaped metal patch surrounded with the slotted square-shaped metallic patches and of 9×9 meta-atoms. The absorber is typically developed in S- and C- bands with resonant frequencies 3.06 GHz, 3.9 GHz, and 5.97 GHz. The absorption is near unity which persists over a wide angle of incidence. The experimental results are in close agreement within 2% with the simulations results.**

***Index Terms*—Energy harvesting, Near unity absorptance, Metasurface, Triple-band absorber**

I. Introduction

WIRELESS electronic devices acquire control over human lives from working smarter to living in smart houses, from small businesses to the medical industries [1-3]. Most of the wireless devices consist of low-power circuits and are placed far from the power supply which restricts us to use energy harvesting methods for powering the device. But the energy harvesting from ambient sources such as thermal, mechanical, and solar energies is limited due to its inaccessibility, high maintenance cost, expansive implementation, and environmental problems [3]. The electromagnetic (EM) waves can also be used as an ambient source for energy harvesting because wireless technology such as smart devices, wifi routers, etc. are available everywhere nowadays [3]. The EM waves are accessible, inexpensive, and do not need to replace (like a battery) from the electronic wireless devices. The EM wave harvester store the energy from the ambient EM wave and provides this energy to low-power electronic devices. The metasurface absorber is an excellent candidate for the EM wave harvester in the future wireless technology owing to its efficient absorbing ability, cost-effectiveness, miniaturization, and being environmentally friendly [3, 4]. The efficiency of the energy harvester can be increased by employing the near unity metasurface absorber.

The metamaterials and metasurfaces (two-dimensional equivalent of bulk metamaterials) exhibit unusual electromagnetic properties in exploiting the propagation of light as well as the amplitude, phase, and polarization state through proper control of structural combinations [5-7]. A metasurface contains a periodic arrangement of the meta-atoms along two mutually perpendicular directions maintaining sub-wavelength periodicity. These meta-atoms act as resonators and can be designed by using various methods like the pixelated concept, split-ring-resonators (SRRs), crosses, etc. [8-10]. The metasurface with various designs of the meta-atoms has been used for polarization conversion, absorbers, antennas, and filters [10-13]. A metasurface absorber can also be used for sensing the environment [14]. A single-band metasurface absorber has a limitation of narrow bandwidth, therefore, there is a requirement of the multiband metasurface absorbers for energy harvesting.

To achieve a multi-band metasurface absorber generally, two methods are used; first layered structure and second coplanar structure [15, 16]. The layered structure possesses high absorptivity but is difficult to realize due to its complex design [17]. On the contrary, the coplanar structures are easy to fabricate and by employing several resonating structures, high absorptivity and multiband absorption can be achieved. Till date, several triple-band metasurface absorbers have been implemented [16, 18-20]. In 2013, The square-shaped closed ring resonator on FR-4 was used for the triple-band absorption with absorptance peaks 94.98%, 87.10%, and 94.06% which was less than 95% in all three bands [16]. Similarly, in 2016, novel square-shaped closed-loop resonators were used for absorptance in S-, C-, and X- bands with 99% absorptivity, but the designed structure of the meta-atom was very complex [18]. A combination of T-shaped and square-like meta-atom was proposed in 2018 [19] for a triple-band absorber, but in this metasurface, not only the design of meta-atom is complex but also only one absorption peak has 99% absorptivity others two

Rajan Agrahari, Email: rajan.ec@nitp.ac.in
Satyesh Singh, Email: satyeshs.ug18.ec@nitp.ac.in
Diptiranjan Samantaray, Email: drsamantaray.rs.ece17@iitbhu.ac.in
Bambam Kumar, Email: bambam.ec@nitp.ac.in
Somak Bhattacharyya, Email: somakbhattacharyya.ece@iitbhu.ac.in
Manpuran Mahto, Email: mmahto@nitp.ac.in
Pradip Kumar Jain, Email: pkjain@nitp.ac.in

* Corresponding Author
[1] Department of Electronics and Communication Engineering, National Institute of Technology Patna, Patna-800005, Bihar, INDIA.
[2] Department of Electronics Engineering, Indian Institute of Technology (BHU) Varanasi, Varanasi-221005, Uttar Pradesh, INDIA.

have 95% and 97% absorptivity. In 2019, a very complex structure was designed for the triple-band absorber with an absorptivity of 91.6%, 99.6%, and 99.8% [20].

Therefore, triple-band metasurface absorbers suffer from either absorptivity less than 95% or a complex design of the meta-atom. It is still highly desirable to design a polarization-insensitive triple-band metasurface absorber with absorptivity of more than 99% adapting a simple meta-atom design that also offers easy fabrication. In this manuscript, a triple-band polarization-insensitive metasurface absorber is proposed using a cross-shaped metal patch surrounded with a slotted square metal patch at the top layer designed over FR4 dielectric backed by metal which shows near-unity absorptance maintaining ultra-thin feature in S- and C-bands. The numerical simulation results illustrate near unity absorptivity typically at 3.06 GHz, 3.9 GHz, and 5.97 GHz. The designed metasurface is fabricated and the experimental results are within 2% agreement with the simulation results.

II. THEORY

The schematic of the meta-atom for the triple-band metasurface absorber is depicted in Fig. 1(a). The metasurface is infinitely extended along the *xy* plane and along the z-direction the wave is incident. The metasurface is bi-periodic in *xy* plane, with each meta-atom taken to be a square of side L in that plane. The proposed meta-atom is a three-layer structure with a low-loss dielectric FR-4 substrate (relative permittivity $\epsilon_s = 4.3(1 + 0.02i)$) as a middle layer and a metallic copper layer with a conductivity 5.8×10^7 S m^{-1} as a bottom layer. The top layer of the meta-atom consists of a composite resonator which includes a cross-shaped copper patch surrounded with the slotted square ring copper patch. The dielectric substrate thickness is $t_s = 2.2$ mm. The thickness of the metallic layer at the top and bottom is $t_m = 0.035$ mm which is several times larger than the skin depth to prevent propagation through the metasurface. All corners in this setup are aligned with Cartesian coordinate system (x, y, z), with $z = 0$ being the front plane and $z = -2t_m - t$ is the bottom plane.

The front plane of the metasurface is illuminated by the propagation of a normal incident plane wave along the z-direction with its electric field phasor is given by

$$\mathbf{E_i} = \left[E_x \hat{\mathbf{u}}_\mathbf{x} + E_y \hat{\mathbf{u}}_\mathbf{y} \right] \exp\left(jk_0 z \right) \tag{1}$$

where, E_x and E_y are the amplitude, $\hat{\mathbf{u}}_\mathbf{x}$ and $\hat{\mathbf{u}}_\mathbf{y}$ are the unit vector along x and y axis. Here, the free space wavenumber is denoted with $k_o (= 2\pi/\lambda_0)$ and λ_0 is the free-space wavelength. The phasor form of the reflected electric field can be written as a doubly infinite series of Floquet harmonics under the condition of metasurface periodicity along the x and y axes [8]:

$$\mathbf{E_r} = \sum_m \sum_n \left\{ \left[\left(R_{xx}^{m,n} E_x + R_{xy}^{m,n} E_y \right) \hat{\mathbf{u}}_\mathbf{x} + \left(R_{yx}^{m,n} E_x + R_{yy}^{m,n} E_y \right) \hat{\mathbf{u}}_\mathbf{y} \right] \exp\left[\frac{j(mx+ny)2\pi}{L} \right] \exp\left(-j\beta^{m,n} z \right) \right\} \tag{2}$$

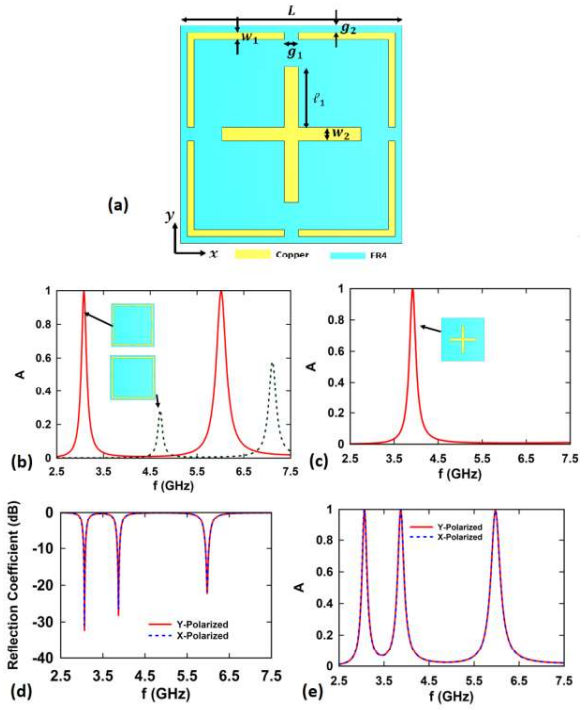

Fig. 1. (a) Schematic of the top view of the meta-atom; (b) the spectra of A delivered by square ring patch with and without slot; (c) the cross shape patch adding an extra peak on spectra of A with two peaks by slotted square ring shape patch. (d) Reflection coefficients response of the proposed triple-band metasurface absorber; (e) the spectra of A delivered by the meta-atom.

where the wavenumbers

$$\beta^{m,n} = \sqrt{k_0^2 - \left(\frac{2\pi}{L} \right)^2 \left(m^2 + n^2 \right)} \tag{3}$$

m and n are the set of all integers; $R_{xx}^{m,n}$ and $R_{yy}^{m,n}$ are co-polarized reflection coefficients (x to x or y to y); $R_{yx}^{m,n}$ and $R_{xy}^{m,n}$ are cross-polarized reflection coefficients (x to y or y to x) and L is the side length of meta-atom.

The reflection coefficients in (2) include both specular and non-specular reflections depending on the value of m and n. The non-specular reflection is mainly caused by the excitation of higher-order modes which depends on the frequency of operation and angle of incidence of electromagnetic waves. The electric field for specular reflection coefficient can be calculated by putting $m = 0$ and $n = 0$ in Eq. (2), whereas the remaining values of m and n represent the electric fields for non-specular reflection coefficients. In our proposed design, the side length of the meta-atom $L < \lambda_c$, where λ_c is the lowest operational value of λ_0. Therefore, the wavenumber $\beta^{m,n}$ in Eq. (3) will be real for $m = 0$ and $n = 0$. The electric field phasor for specular reflection is given by

$$\mathbf{E_r} \to \left[\left(R_{xx}^{0,0} E_x + R_{xy}^{0,0} E_y \right) \hat{\mathbf{u}}_\mathbf{x} + \left(R_{yx}^{0,0} E_x + R_{yy}^{0,0} E_y \right) \hat{\mathbf{u}}_\mathbf{y} \right] \exp(-j\beta^{0,0} z) \tag{4}$$

as $z \to \infty$.

The absorptance (A) of the metasurface absorber is given by

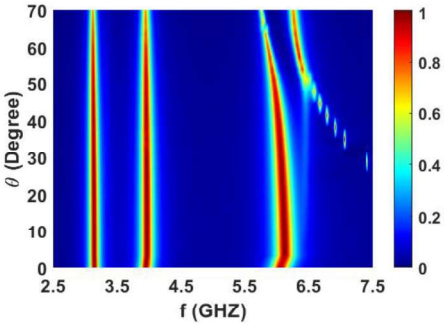

Fig. 2: The spectra of A delivered by the proposed triple-band metasurface absorber for $\theta \in [0^\circ,\ 70^\circ]$.

$$A = \begin{cases} 1 - \left|R_{xx}^{0,0}\right|^2 - \left|R_{yx}^{0,0}\right|^2 & \text{for } x\text{–polarized wave} \\ 1 - \left|R_{xy}^{0,0}\right|^2 - \left|R_{yy}^{0,0}\right|^2 & \text{for } y\text{–polarized wave} \end{cases}. \quad (5)$$

The reflection and transmission from the proposed metasurface are simulated by using simulation software CST Microwave Studio 2021 [21]. The periodic boundary conditions have been employed in the design with a perfect match layer is used above and below the structure to prevent any unwanted reflection from the boundaries.

III. Design Principle

The metasurface absorber is designed according to the various applications for example multiband absorber with near-unity absorptance is required to achieve high output power for the energy harvesting. To design a near-unity multiband absorber, the simple shape and number of resonators in the meta-atom must be taken into consideration. Moreover, the operating frequency decides the size of the meta-atom. The independence of the polarization and incidence angle is also considered while we design the metasurface absorber.

The absorber design can be understood with the impedance matching theorem. If the effective impedance of the metasurface absorber (Z_e) matched with the surrounding impedance (Z_s) then no reflection ($\Gamma(\omega) \approx 0$) takes place from the designed metasurface. The effective impedance of a metasurface can be calculated from reflection (R) and transmission (T) coefficients as [3]

$$Z_e = \sqrt{\frac{(1+R)^2 - T^2}{(1-R)^2 - T^2}}. \quad (6)$$

$$\text{Here, } |R|^2 = \begin{cases} |R_{xx}|^2 + |R_{yx}|^2 & \text{for } x-\text{polarized wave} \\ |R_{xy}|^2 + |R_{yy}|^2 & \text{for } y-\text{polarized wave} \end{cases}.$$

Further, in order to make zero transmission ($T \approx 0$) for trapping the EM wave into the metasurface, a metal layer on the bottom of the metasurface is required.

Initially, we fixed the parameters $L = 32$ mm, $g_2 = 1$ mm, and $w_1 = 1$ mm to patterned a square ring patch on the FR-4 substrate and plotted the absorptance (A) spectra using Eq. (5). in Fig. 2(a). The square ring structure does not produce any absorptance peak

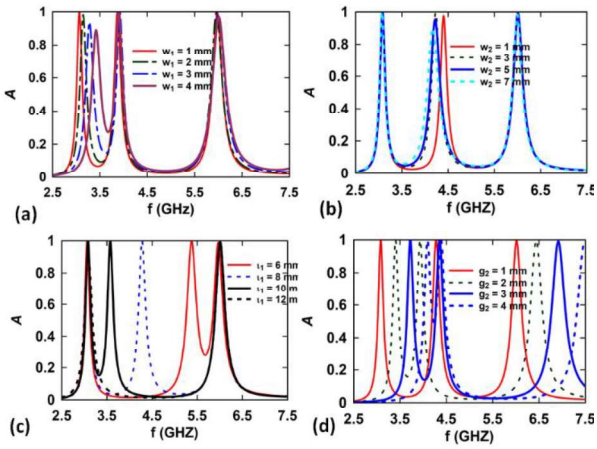

Fig. 3: Effect of various geometrical parameters on A.

($A > 0.9$), but the incorporation of rectangle shape slots of size $g_1 = 2$ mm in the square ring produces two absorptance peaks at 3.08 GHz and 6.00 GHz (see Fig. 1(b)). In order to include one more absorptance peak we studied the cross-shape patch with dimensions $w_2 = 2$ mm, and $\ell_1 = 9$ mm patterned on the FR-4 at the center of the meta-atom. The cross-shape patch alone produces an absorptance peak at 3.93 GHz as shown in Fig. 1(c). Therefore, a triple-band absorber is designed by integrating the cross-shape patch with the slotted square ring patch.

IV. Results and Discussion

Figure 1(d) shows the frequency response of proposed metasurface absorber. The reflection coefficient is observed below 10 dB at frequencies 3.06 GHz, 3.87 GHz, and 5.98 GHz. The absorptance of the meta-atom is calculated by using Eq. (5) and plotted in Fig. 1(e). Approximately 100% absorptance is obtained at the resonant frequencies 3.06 GHz, 3.9 GHz, and 5.97 GHz. The absorption peaks at three distinct frequencies are produced by the combination of slotted square ring and cross pattern patches as revealed from Fig. 1(b, c). Therefore, in the proposed metasurface the first and third peaks are primarily formed by the slotted square ring while the second absorption peak is due to the cross-pattern structure.

The absorption performance of the proposed metamaterial absorber has been studied for the oblique incidence of the EM waves; i.e.,

$$\mathbf{E_{inc}} = E_0 \exp[jk_0(x\sin\theta + z\cos\theta)]\,(\hat{\boldsymbol{x}}\cos\theta - \hat{\boldsymbol{z}}\sin\theta) \quad (7)$$

with $\theta \in [0^\circ, 70^\circ]$. For $f > 4.5$ GHz, when $\theta > 15^\circ$ nonspecular modes started contributing to the reflected wave energy which results in instability of the third peak of A with θ. Figure 2 shows the A spectra delivered by the proposed metasurface under an oblique angle of incidence. We can observe that the first two peaks of A of the proposed metasurface is mostly unaffected by the angle of incidence and it shows approximately 100% A at 3.06 GHz and 3.9 GHz for θ up to 45°. Furthermore, A peak at 5.97 GHz is unstable for most of the θ and its magnitude decreases with peaks shifted towards lower frequency as θ increase. It is important to note that, the

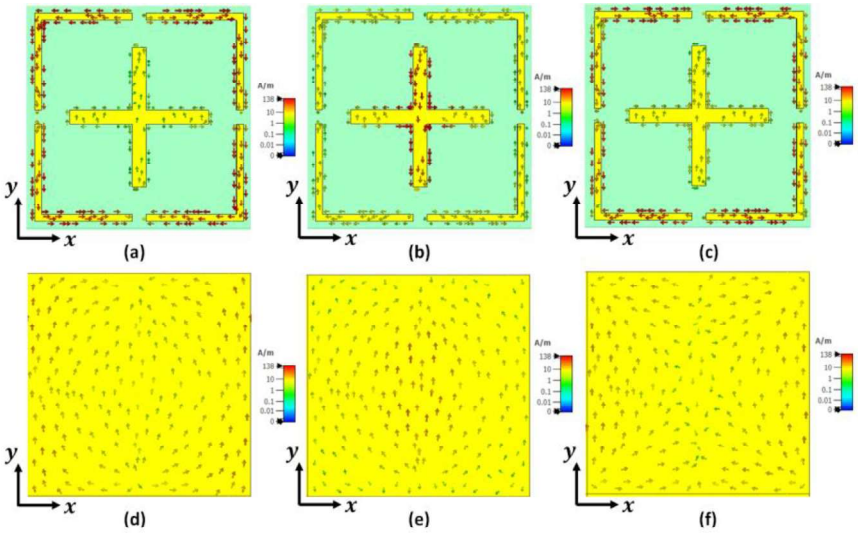

Fig. 4: Vector plots of the surface electric current density on the (a, b, c) front and (b, c, d) back planes of the designed meta-atom at (a, d) 3.06 GHz, (b, e) 3.9 GHz, and (c, f) 5.97 GHz.

Table I: Comparison of existing triple-band metasurface absorber designed with proposed design

Ref.	Meta-atom Structure (top layer)	Substrate used	Absorption A (%)	Absorption Frequency (in GHz)	Meta-atom size	Thickness
[16]		FR4	94.98 87.1 94.06	5.22 7.44 10.02	18 × 18 mm (0.313 λ_0)	1 mm (0.017 λ_0)
[18]		FR4 Epoxy	99.67 97.52 99.84	3.1 4.6 9.5	15 × 15 mm (0.154 λ_0)	1.6 mm (0.016 λ_0)
[19]		FR4 epoxy	95 97 99	5.8 9.52 11.97	9.3 × 9.3 mm (0.18 λ_0)	1 mm (0.019 λ_0)
[20]		FR4	91.6 99.6 99.8	3.44 6.36 11.51	12 × 12 mm (0.137 λ_0)	0.8 mm (0.009 λ_0)
[25]		Polyimide	92.5 94.9 88.6	101.25 108.75 129	1.46 × 1.46 mm (0.492 λ_0)	50 μm (0.017 λ_0)
[26]		FR4 epoxy	99.01 97.18 99.53	8.98 13.86 15.04	10 × 10 mm (0.299 λ_0)	0.8 mm (0.024 λ_0)
Proposed work		FR4	99.94 99.84 99.50	3.06 3.9 5.97	32 × 32 mm (0.32 λ_0)	2.2 mm (0.022 λ_0)

fourth A peak is observed when $\theta > 30°$ consistent with the contribution of the nonspecular modes to the reflected wave energy for higher frequencies. Our proposed triple-band metasurface absorber shows the identical response for the y-polarized wave due to the symmetrical design incurred in the copper patch.

The performance of the proposed triple-band metasurface absorber is analyzed by calculating the effect of various geometrical parameters on A, as shown in Fig. 3. The first peak of A is highly affected by the width of the slotted square shape copper patch (w_1) but it does not affect the second and third A peaks. The amplitude of A is decreased and shifted to a higher frequency as the width of the slotted square shape patch increases (see Fig. 3a). The second A peak can be altered by varying the width (w_2) and length (ℓ_1) of the cross-shape patch as shown in Figs. 3(b) and (c). Further, the first and third peaks are not affected by the dimensional parameters of the cross-shape patch as found consistent with the results shown in Fig. 2. Finally, the effect of gap (g_2) between the meta-atom side and slotted square shape patch is calculated and shown in Fig. 3(d). The first and third peaks undergo blue-shift when g_2 is increased from 1 mm to 4 mm but the second peak is invariant with respect to the variation of g_2.

To explain the physical mechanism of absorptance, we determined the surface electric current density $\mathbf{J_s} = \hat{\mathbf{z}} \times \mathbf{H}$ on the front and back planes of the metasurface at 3.06 GHz, 3.9 GHz, and 5.97 GHz as shown in Fig. 4. In a metasurface, an electric resonance is generated when $\mathbf{J_s}$ at the front and back planes are parallel to each other while a magnetic resonance is formed when $\mathbf{J_s}$ at the front and back planes are opposite to each other [22-25]. In Fig. 4, the directions of $\mathbf{J_s}$ at the front and back planes are anti-parallel to each other at the places where

the magnitude of $\mathbf{J_s}$ is high. Therefore, the absorption peak is primarily caused by magnetic resonance. For the resonance frequencies 3.06 GHz and 5.97 GHz, the magnitude of the $\mathbf{J_s}$ is observed high at the slotted square ring and low at the cross-pattern structure (see Fig. 4(a), (c), (d), and (f)). This indicates that the first and third resonance is mainly caused by the slotted square ring and is consistent with the structural analysis results in Fig. 1. Similarly, Fig. 4(b) and (e) show that at frequency 3.9 GHz the magnitude of $\mathbf{J_s}$ is high at the cross structure. Furthermore, the direction of $\mathbf{J_s}$ at front and back plane are opposite to each other. Therefore, the second absorptance peak is due to cross structure and is formed by magnetic resonance.

Table 1 shows the comparison of the previously reported triple-band metasurface absorber with the proposed design. It can be observed that the proposed design structure is very simple in comparison to other previous reported works which makes the device easy to fabricate. Further, the proposed design offers near-unity absorption for all three bands which was not achieved with the previously reported works.

V. Experimental Result

A prototype of the triple-band metasurface absorber has been fabricated with 9×9 unit cells on top of an FR-4 substrate having a thickness of 2.2 mm and the dimension of 288 mm $\times$ 288 mm by using a standard lithography technique as shown in Fig. 5(a, b). The experimental setup for measuring the reflection from the fabricated sample is shown in Fig. 5(c, d, e). The fabricated sample is placed at a far-field distance of the horn antenna and fixed on a wooden stand as shown in Fig. 5c. The transmitting and receiving horn antennas are connected with the vector network analyzer KEYSIGHT FieldFox Microwave Analyzer (5 kHz – 44 GHz) and placed in front of the sample within the anechoic chamber (see Fig. 5(d) and (e)).

First, the reference level for the measurement is fixed by measuring the reflection from a copper sheet, identical to the dimension of the fabricated sample. Then, the reflection from the fabricated sample is measured. The difference of the reflection from the fabricated sample with the reflection from the identical copper surface gives the actual reflection from the fabricated sample. The reflection coefficient measurement with VNA and the comparison of the experimentally measured results with the simulated results are shown in Fig. 5(f, g). The resonant frequencies for the fabricated sample are obtained at 3.05 GHz, 3.87 GHz, and 5.89 GHz. The first and second resonant frequencies are exactly matched with the simulated results. However, the third resonant frequency of the fabricated sample is shifted to a lower frequency when compared with the simulated results. This is due to the imperfection in the fabricated sample and measurement accuracy. Here, the amplitudes of the reflection coefficient at all three resonant frequencies are below -25 dB, which indicates a near-unity absorptivity at these resonance frequencies.

VI. Conclusion

A simple design of the reflective type polarization-independent near unity triple-band metasurface absorber for energy harvesting applications has been presented in this paper. The designed absorber is capable of absorbing near-unity electromagnetic waves in all three bands within S- and C- bands

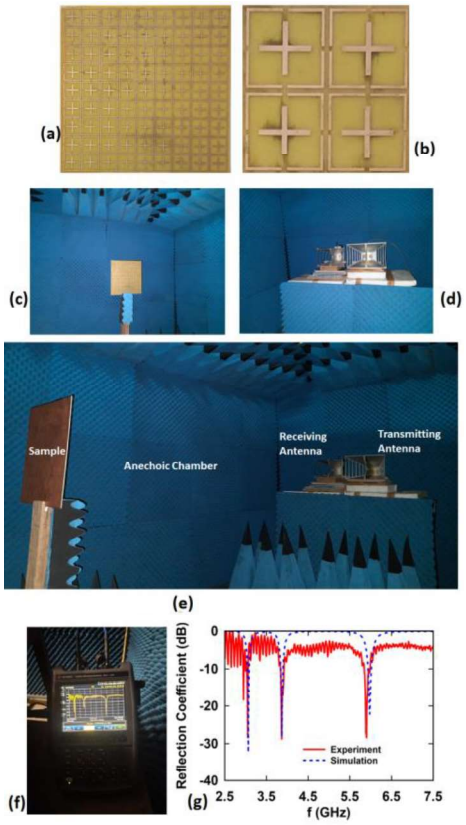

Fig. 5: The prototype of the metasurface absorber fabricated by the standard photolithography method on FR4 dielectric substrate with a metal copper layer on top and bottom side; (a) top view, and (b) enlarged view of 2×2 meta-atom; (c, d, e) experimental setup; (f) reflection coefficient measurement using VNA; and (g) comparison of the simulated and experimental results.

with a very small thickness of $0.022\,\lambda_0$. It has been observed that a simple cross-shaped metallic patch surrounded with a slotted square patch shows near unity absorptivity over large incident angles and also independent to polarization. The absorptivity of 99.7%, 99.8%, and 99.2% have been observed at the resonant frequencies of 3.06 GHz, 3.9 GHz, and 5.97 GHz, respectively. The physical mechanism of the absorptance has been discussed with the electric surface current density at the front and back plane of the proposed meta-atom. The extremely good traits of the proposed metasurface absorber can be utilized in energy harvesting, electromagnetic shielding, and communication.

References

[1]. E. Sisinni, A. Saifullah, S. Han, U. Jennehag, and M. Gidlund, *IEEE Trans. Ind. Informatics*, **14** (11), 4724–4734, 2018.

[2]. I. Makhdoom, M. Abolhasan, J. Lipman, R. P. Liu, and W. Ni, *IEEE Commun. Surv. Tutorials*, **21** (2), 1636–1675, 2019.

[3]. M. Amiri, F. Tofigh, N. Shariati, J. Lipman, and M. Abolhasan, *IEEE Internet Things J.*, **8** (6), 4105–4131, 2021.

[4]. N. Muhammad, T. Fu, Q. Liu, X. Tang, Z. L. Deng, and Z. Ouyang, *Mater.* **11** (11), 2315, 2018.

[5]. H. T. Chen, A. J. Taylor, and N. Yu, *Reports Prog. Phys.*, **79** (7), 076401, 2016.

[6]. S. B. Glybovski, S. A. Tretyakov, P. A. Belov, Y. S. Kivshar, and C. R. Simovski, *Phys. Rep.*, **634**, 1–72, 2016,

[7]. G. Sharma, A. Lakhtakia, S. Bhattacharyya, and P. K. Jain, *Appl. Opt.* **59**(31)*,* 9673-9680, 2020.

[8]. R. Agrahari, A. Lakhtakia, P. Kumar Jain, and S. Bhattacharyya, *J. Electromagn. Waves Appl.* **36**(7), 1008-1019, 2021.

[9]. G. Singh, A. Bhardwaj, K. V. Srivastava, J. Ramkumar, and S. A. Ramakrishna, *Appl. Phys. A Mater. Sci. Process.* **127**(11), 1-9, 2021.

[10]. S. K. Ghosh, S. Das, and S. Bhattacharyya, *Appl. Opt.* **60**(36)*,* 11247-11255, 2021,

[11]. S. Bhattacharyya, S. Ghosh, and K.V. Srivastava, *Radio Sci.*, **52**(11), 1395–1404, 2017.

[12]. D. Samantaray and S. Bhattacharyya, *IEEE Trans. Antennas Propag.*, **68**, 9, 6548–6556, 2020.

[13]. M. T. Nouman, J. H. Hwang, M. Faiyaz, K. J. Lee, D. Y. Noh, and J. H. Jang, *Opt. Express,* **26** (10), 12922–12929, 2018.

[14]. B. X. Wang, Y. He, P. Lou, and W. Xing, *Nanoscale Adv.*, **2** (2), 763–769, 2020.

[15]. Z. Chen, H. Chen, H. Jile, D. Xu, Z. Yi, Y. Lei, X. Chen, Z. Zhou, S. Cai and G. Li, *Diam. Relat. Mater.*, **115**, 108374, 2021.

[16]. S. Bhattacharyya, S. Ghosh, and K. V. Srivastava, *J. Appl. Phys.*, **114** (9), 094514, 2013.

[17]. S. Bhattacharyya, S. Ghosh, D. Chaurasiya, and K. V. Srivastava, *Appl. Phys. A Mater. Sci. Process.*, **118** (1), 207–215, 2015.

[18]. S. K. Sharma, S. Ghosh, and K. V. Srivastava, *Appl. Phys. A Mater. Sci. Process.*, **122** (12), 1–8, 2016.

[19]. R. Asgharian, B. Zakeri, and O. Karimi, *AEU - Int. J. Electron. Commun.*, **87**, 119–123, 2018.

[20]. K. Muthukrishnan and V. Narasimhan, *Plasmonics*, **14** (6), 1983–1991, 2019.

[21]. CST Studio Suite, CST Microwave Studio, 2021. http://www.cst.com.

[22]. Y. Zhao, B. Qi, T. Niu, Z. Mei, L. Qiao, and Y. Zhao, *AIP Adv.*, **9** (8), 085013, 2019.

[23]. X. Gao, X. Han, W. P. Cao, H. O. Li, H. F. Ma, and T. J. Cui, *IEEE Trans. Antennas Propag.*, **63** (8), 3522–3530, 2015.

[24]. X. Ma, Z. Xiao, and D. Liu, *J. Mod. Opt.*, **63 (**10), 937–940, 2015.

[25]. G. Deng, T. Xia, J. Yang, and Z. Yin, *IET Microwaves, Antennas Propag.*, **12** (7), 1120–1125, 2018.

[26]. T. Wu, Y. M. Ma, J. Chen, and L. L. Wang, *Int. J. RF Microw. Comput. Eng.*, **30** (9), e22314, 2020.